PCCP

Accepted Manuscript

ROYAL SOCIETY OF CHEMISTRY

www.rsc.org/pccp

Water transport in the nano-pore of calcium silicate phase: reactivity, structure and dynamics

Dongshuai HOU[a] Zongjin LI[b] Tiejun ZHAO[c] Peng ZHANG[d]

a. Assistant Professor; Qingdao Technological University(Cooperative Innovation Center of Engineering Construction and Safety in Shandong Blue Economic Zone), Qingdao, China; Corresponding author, telephone number: +85267636710; email address: dhou@ust.hk ; monkeyphil@126.com

b. Professor; Qingdao Technological University(Cooperative Innovation Center of Engineering Construction and Safety in Shandong Blue Economic Zone), Qingdao, China; zongjin@ust.hk

c. Professor, Qingdao Technological University(Cooperative Innovation Center of Engineering Construction and Safety in Shandong Blue Economic Zone), Qingdao, China; ztjgp@263.net

d. Associate Professor，Qingdao Technological University(Cooperative Innovation Center of Engineering Construction and Safety in Shandong Blue Economic Zone), Qingdao, China; zhp0221@163.com

Abstract

Reactive force field molecular dynamics was utilized to simulate the reactivity, structure and dynamics of water molecules confined in calcium-silicate-hydrate (C-S-H) nano-pores of width 4.5 nm. Due to the highly reactive C-S-H surface, hydrolytic reactions occur in the solid-liquid interfacial zone, and partial surface adsorbed water molecules transforming to the Si-OH and Ca-OH groups are strongly embedded in the C-S-H structure. Due to the electronic charge difference, the silicate and calcium hydroxyl groups have binomial distributions of the dipolar moment and water orientation. While the Ca-OH contributes to the O_w-downward orientation, the O_{NB} atoms in the silicate chains prefer to accept H-bonds from the surface water

molecules. Furthermore, the defectives silicate chains and solvated Ca_w atoms near the surface contribute to the glassy nature of the surface water, with large packing density, pronounced orientation preference, and distorted organization. The stable H-bonds connected with the Ca-OH and Si-OH groups also restrict the mobility of the surface water molecules. The significant reduction of the diffusion coefficient matches well with the experimental results obtained by NMR, QENS and PCFR techniques. With increasing distance from the channel, the structural and dynamical behavior of the water molecules vary and gradually translate into bulk water properties at distances of 10~15 Å from the liquid-solid interface.

Key words: Reactive force field, H-bonds, diffusion coefficient, dipolar moment, hydrophilic surface, water dissociation

1. Introduction

Water covers 71% of the earth's surface and is a critical source for all forms of life. As a vital component in biological bodies and manufactured products, water is essential for various chemical reactions ranging from the photosynthesis of plants, the digestive process of animals and the hydration reaction in the cement based materials. In biological, industrial and geological systems, water molecules confined in the nano-pores have been extensively investigated. From water molecules in biological cells to molecules diffusing between the gel pores in the cement hydrate, water molecules, influenced by the geometrical and electronic confinement, demonstrate dramatically the different properties from the bulk counterpart.

Calcium silicate hydrate (C-S-H), one of the main hydration products of cement-based material, is a porous gel with gel pores characterized in size from 0.5 nm to 10 nm, where the water and ions can diffuse. In this respect, C-S-H gel can be utilized to study the chemical and physical properties of confined water molecules. The water

and ion diffusion in the C-S-H gel determines the strength, creep, shrinkage, chemical and physical reactivity of cementitious materials. The properties of the water confined in gel pores or in the vicinity of C-S-H surfaces have been studied by various experimental techniques. By using the ^{1}H nuclear magnetic resonance (NMR) (Wang, et al., 1998) (Rakiewicz, et al., 1998) (Greener, et al., 2000), the water in C-S-H gels was distinguished into three types: chemically bound water that is incorporated into the structure and forms strong chemical bond with the calcium silicate structure, physical bound water that is deeply adsorbed near the surface and capillary water that is not bound and diffuses freely in the capillary pores. Furthermore, the quasi-elastic neutron scattering (QENS) technique (Bordallo, et al., 2006) characterizes the different water types by quantitatively using the diffusion coefficient. The unbound water molecules in the pores move at a fast rate (diffusion coefficient~ 10^{-9} m^2/s), while the water molecules confined in the gel pores diffuse slowly (~10^{-10} m^2/s). Similarly, hydration water dynamics in tri-calcium silicate (C_3S) pastes by QENS also showed that the diffusion coefficient of surface adsorbed water molecules decreases from 4×10^{-9} m^2/s to 4×10^{-10} m^2/s after two days hydration. A proton field cycling relaxometry approach (PFCR) was also developed to investigate the dynamic properties of the water molecules bound in the C-S-H surface (Korb, et al., 2007). During approximately 1 ns, the diffusion coefficient of the water molecules in the C-S-H gel pore surface is about 1/60 of the bulk water value (0.4×10^{-10} m^2/s). Furthermore, in the respect of the interaction between ions and the C-S-H surface, the ^{35}Cl NMR relaxation methods (Yu & Kirkpatrick, 2001) and a two-site exchange model have been proposed to study the in situ molecular-scale structural and dynamical properties of chloride binding on a C-S-H mineral analogue in contact with aqueous chloride solutions. The low fraction of the binding chloride ions on the surface implies the weak Cl ions binding capacity of the C-S-H surface.

However, investigating the water structure and dynamics by experiment alone is challenged by some limitations, such as the material purity and instrument accuracy at the relevant lengths and timescales. Computational methods can help to interpret the

experimental results and play a complementary role in understanding the structural and dynamic properties at the molecular level. Molecular dynamics (MD), a force field based computational method, is able to give a more quantitative illustration of the structure, dynamics and energy of solid-liquid interfaces. Kalinichev (2007) (Kalinichev, et al., 2007), whose group developed the ClayFF force field (Cygan, et al., 2004) , introduced the force field model to a cement system and investigated multi-phases in the cement based material. In light of the mineral interface properties, MD simulation was performed to study the water confined between the brucite layers. In addition to the water/cement interface study, they also performed MD simulation to study the structure and dynamic behavior of chloride at the interface between cement hydrate and an ions solution (Kalinichev & Kirkpatrick, 2002). Good descriptions, both in the structure and the dynamic properties of various cement phases, can confirm the suitability of the ClayFF force field in cement material simulation. Nevertheless, the MD simulation is based on the C-S-H analogues, tobermorite and jennite, which cannot completely represent the complicated structural features of C-S-H gel. With increasing knowledge of the molecular structure of C-S-H, water confined in the interlayer region has been extensively investigated, indicating that the glassy nature of water restricted by the less than 1 nm of confinement (Youssef, et al., 2011).

So far, there have been few investigations of the water confined in the C-S-H meso-pores (2 nm~10 nm) that are widely distributed in the cement hydrate. In our study, molecular simulation by the reactive force field is first utilized to simulate the water molecules confined in the C-S-H gel pore. It is worth noting that the solid-liquid interface, described by the reactive force field, can reflect the chemical response of water molecules confined in the gel pores, which depicts more realistic behavior than that obtained from empirical force field approaches such as CSHFF and ClayFF. Additionally, the density profiles, atomic trajectories, diffusion coefficients and H-bond networks were employed to characterize the structural and dynamic behavior of the water molecules in the nano pores in a systematic style. The

simulations aim to give insights on the molecular structure, dynamic motion and reactive interaction between the water and the C-S-H surface.

2. Simulation method

2.1 Reaction force field

The Reactive force field (ReaxFF), developed by van Duin et al (van Duin, et al., 2003), is utilized to simulate water transport in the calcium silicate phase. The Reactive force field provides an advanced description of the interaction between Ca, Si, O and H atoms in the C-S-H gel. The short-range interactions for the ReaxFF force field are determined by a bond length-bond order scheme so that the bonds can be broken and formed, with the potential energy transforming into a smooth state (Brenner, et al., 2002). On the other hand, the long-range coulombic interactions are determined by a 7^{th} order taper function, with an outer cut off radius of 10 Å. The Reactive Force field has been widely utilized in silica-water interfaces (Leroch & Wendland, 2012), calcium silicate hydrate gel (Manzano, et al., 2013) and nano-crystals (Lau, et al., 2010). The parameters of the force field for Ca, Si, O and H can be directly obtained from previous published reference data (van Duin, et al., 2003).

2.2 C-S-H gel pore model

For the C-S-H gel, the model construction in the present study is based on the procedures that combine the method proposed by Pellenq (Pellenq, et al., 2009) and Manzano (Manzano, et al., 2011). Firstly, the layered analogue mineral of C-S-H, tobermorite 11Å without water, was taken as the initial configuration for the C-S-H model (Murray, et al., 2010). Silicate chains were then broken to match the Q species distribution with Q_1=73.9%, Q_2=21.4% and Q_0=4.7%. The mean silicate chain length

(MCL=2(Q_2/Q_1+1)=2.58) is consistent with the results obtained both from NMR testing (Cong & Kirkpatrick, 1996) and molecular dynamics simulation (Dolado, et al., 2007). It is worth noting that the Q_0 percentage is controlled to less than 5%, also matching well with experimental results (Brough, et al., 1994). Meanwhile, the Ca/Si ratios range from 0.7 to 2.3 with an average value of 1.7. In order to increase the Ca/Si ratio, some of the bridging SiO_2 units were first removed as proposed by Pellenq et al. (Pellenq, et al., 2009). More importantly, some dimmer structures (Si_2O_4) were also removed to satisfy the Q species distribution, especially for the low Q_0 percentage. After omission of the dimmer structure, to maintain charge neutrality, some oxygen atoms in the silicate chains have to remain in the form of dangling atoms. In this way, the dry calcium silicate skeleton can be obtained, as shown in Fig.1a. The C-S-H surfaces are created by cleaving the crystal structure at the center of interlayer region that is parallel to (001) crystallographic plane. As shown in Fig.1a, the C-S-H surface is composed of the Ca_w atoms adsorbed on the defective silicate chains. Then the cleaved C-S-H structures were separated and leave around 4.5 nm space in the interlayer region.

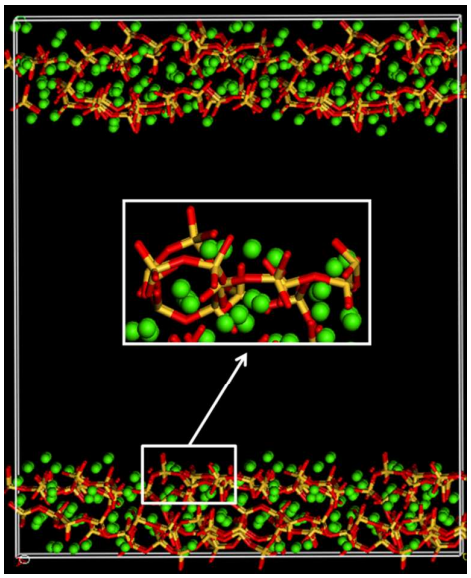

a

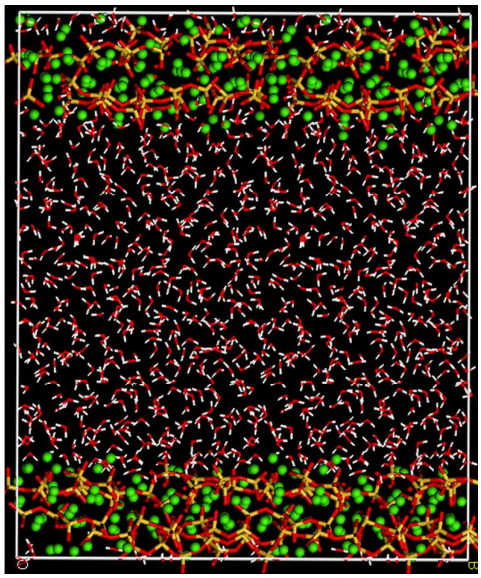

b

Fig.1 a. initial dry gel pore structure; b. saturated C-S-H gel pore after GCMC adsorption

Subsequently, the Grand canonical Monte Carlo (GCMC) method was utilized to investigate the structure of the dry calcium silicate skeleton emerged in water solution (Bonnaud, et al., 2012). The dry sample obtained by the temperature quenching method was utilized for simulation. GCMC simulations determine the properties of the water molecules confined in the calcium silicate system at constant volume V in equilibrium with a fictitious infinite reservoir of liquid bulk water solution, imposing its chemical potential μ=0 eV and its temperature T=300 K (Pellenq, et al., 2009). The simulation process is analogue to water adsorption in the micro-porous phases, such as calcium silicate hydrate and zeolite (Puibasset & Pellenq, 2008).The simulation included 300,000 circles for the system to reach equilibrium followed by 100,000 circles for the production run. For each circle, it was attempted to insert, delete, displace and rotate water molecules 1000 times in the constant volume calcium silica hydrate system. After GCMC adsorption, the saturated C-S-H gel pore is exhibited in Fig. 1b.

Finally, the reactive force field molecular dynamic simulations under constant

pressure and temperature (NPT) for 400 ps give the structures of C-S-H gel at equilibrium states. A further 400 ps NPT run was employed to achieve the equilibrium configuration for structural and dynamic analysis.

3. Results and discussion

3.1 Interface reactivity

As mentioned above, the C-S-H surface is composed of the defective silicate chains and interlayer calcium atoms. The complicated surface resembles the combination of the structural features of both calcium oxide and the amorphous silica glass. Reactive force field can describe the chemical interaction between surface water molecules and the calcium silicate substrate. Water molecules, adsorbed on the neighboring calcium silicate sheets, dissociate and form Ca-OH and Si-OH bonds. As displayed in Fig.2, the continuous decreasing water number and increasing hydroxyl groups indicates the hydroxylation reaction near the C-S-H gel surface. The hydrolytic reaction rate is quite fast; during less than 0.1 ns, about 9.6 % of the water molecules within gel pore dissociate. The dissociation degree is dramatically reduced in compared with the water molecules ultra-confined in disconnected small pore (75 %) and connected large pore (40 %) in the C-S-H gel (pore diameter less than 1 nm) (Manzano, et al., 2011). In this respect, the reaction degree of the confined water molecules is significantly influenced by the size of nano-pore. In current simulation, due to the long distance between up and bottom calcium silicate surfaces, water molecules adsorbed on one C-S-H substrate are not influenced by the other substrate. Hence, the reactivity of gel pore water is not as active as structural water ultra-confined in the interlayer space (less than 1 nm). In addition, as shown in Fig.2, the percentage of Ca-OH is two times larger than the interfacial Si-OH bonds. The relative high Ca-OH/Si-OH ratio at Ca/Si=1.7 is consistent with previous reactive simulation of calcium silicate hydrate gel (Dolado, et al., 2007) and the charge balance method (Cong & Kirkpatrick, 1996).

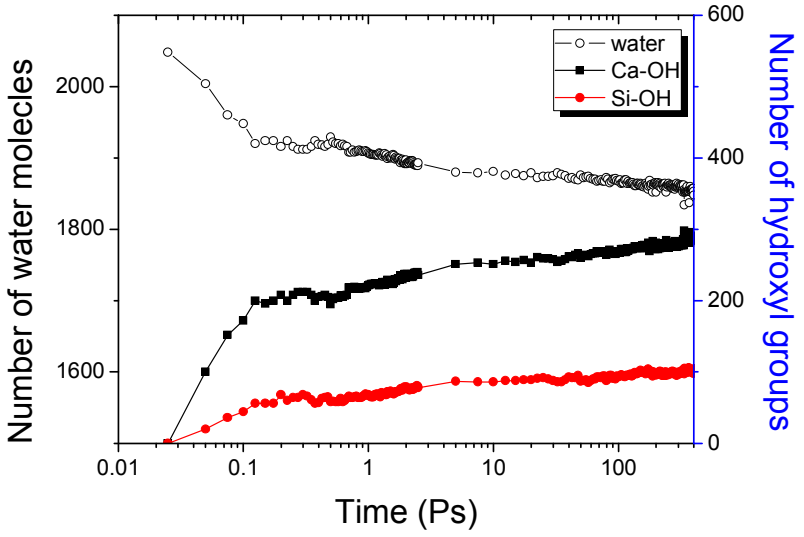

Fig.2 number of the water molecules and hydroxyl groups varies in 400 Ps.

The discrepancies between silicate and calcium hydroxyls mainly result from different hydrolytic reactions which are induced by chemical adsorption on the Si-O site and Ca-O site, respectively. In regard to the former case, the reaction pathway can be illustrated in Fig.3. Initially, as shown in Fig. 3a, the water molecule diffuses and approximates to the non-bridging oxygen (O_{NB}) atom in the silicate chains. Surface adsorbed water molecule donates H-bond connection to the O_{NB} site. Then, Fig.3b shows that due to the strong electronic attraction from the silicate chains, water molecule dissociate into H^+ and OH^-. H^+ ion directly binds to the O_{NB} site and forms the Si-OH bond (Fig.3c). However, as shown in Fig. 3d and Fig. 3e, the OH^- causes further dissociation of water molecules by "borrowing" the proton from neighboring molecules. Finally, the later dissociated OH^- ion explores the attraction from surface Ca atoms and constructs the Ca-OH bonds. It should be noted that the proton transferring from one molecule to another is not necessary to happen. If the dissociated OH^- ion is located near the surface, it can directly diffuse to Ca atoms. The reaction products for chemical adsorption on Si-O^- site are both Si-OH and Ca-OH groups.

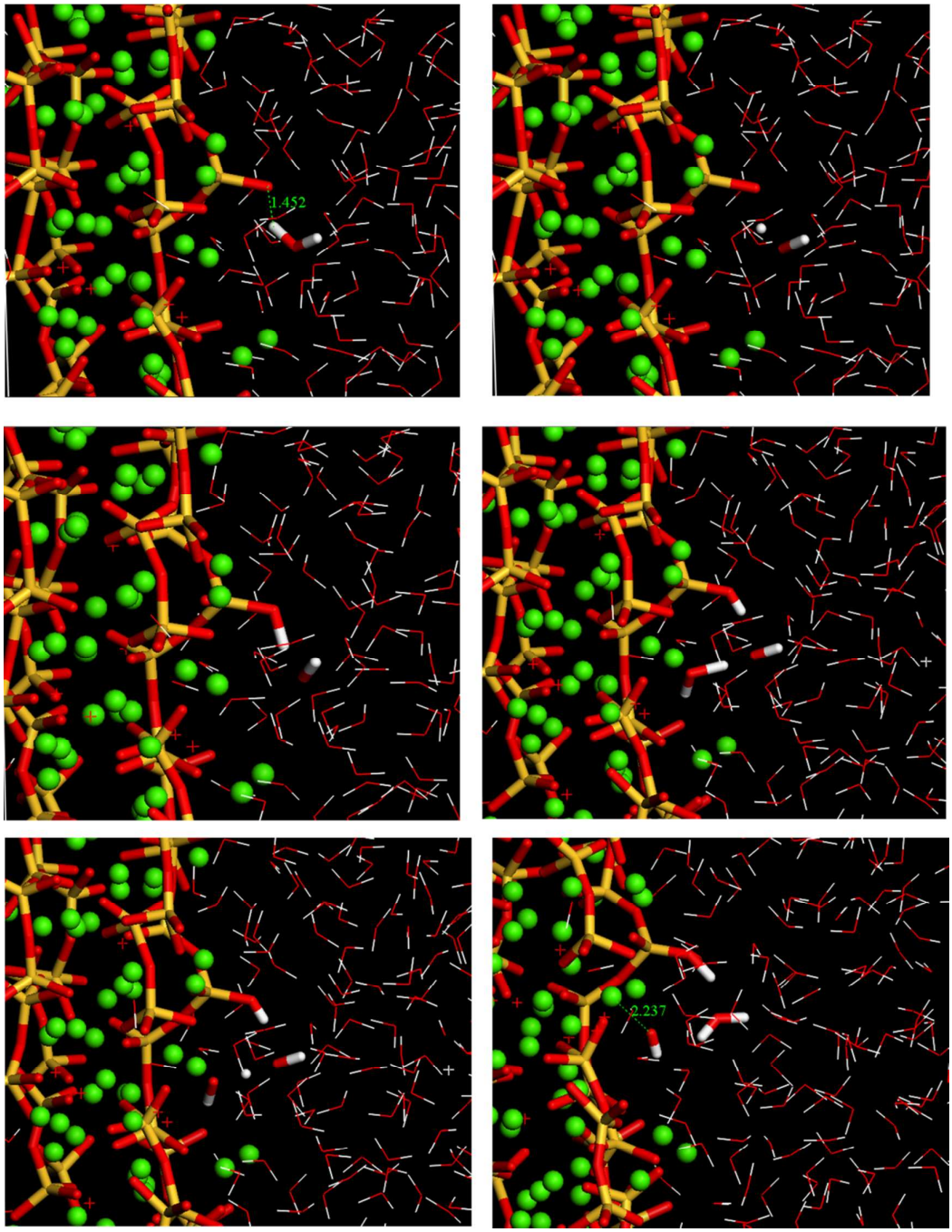

Fig.3 Reaction pathway for the chemical adsorption of water on the Si-O site.

On the other hand, in the surface of the C-S-H gel, H^+ ions in the water molecules not only associate with the O_{NB} atoms in the defective silicate chains, but they also

connect with the dangling oxygen atoms in the calcium sheet due to the elimination of the dimmer structures. As shown in Fig.4, the strong negative charge of the dangling oxygen atoms leads to the hydrolytic reaction of water molecules. Since only disordered Ca-OH groups are produced during the reactions, the percentage of Ca-OH group increases significantly. Furthermore, during the hydrolytic reaction process, as shown in both Fig. 3 and Fig. 4, H^+ ions do not associate with the O_B atoms connected by two silicon atoms and also O_{NB} atoms coordinated with two Ca_s atoms and one silicon atom. The reactivity for water molecules depend greatly on the electronegativity of oxygen atoms in the silicate chains. In previous research, the O_B atoms in the siloxane bond, due to the hydrophobic nature, are hard to associate with the water molecules (Manzano, et al., 2011). Besides, Ca^{2+} ions, the courter ions, which share the negative charge of oxygen atoms, reduce the electronegativity of O_{NB} atoms so that the dissociation reaction is slowed down. The reactivity of different oxygen atoms in the surface follows the sequence: dangling oxygen atoms > non-bridging oxygen atoms > bridging oxygen atoms. The high activity is an important feature to distinguish C-S-H and its mineral analogues such as tobermorite or jennite. The mineral crystal, with infinite long silicate chains, demonstrates slight hydrophobic nature and the H-bonds connection between O_B and water molecule is quite weak. At the interface between water and the C-S-H gel, the disorder influences the reactivity significantly. Dimmer silicate structure, the short chains, account for dominant percentage in the C-S-H gel, which provides large amount of O_{NB} sites in C-S-H surface. As a result, the reactivity is greatly improved.

Despite different hydrolytic reaction mechanisms, both reactions help transform partial surface adsorbed water molecules to the hydroxyl groups strongly embedded in the C-S-H structure. The calcium silicate hydroxyl layers can not only enhance the stability of the interfacial water molecules, but also reduce the activity of the disordered calcium silicate structure. The structural and dynamic properties of hydroxyl layers are further discussed quantitatively in the following sections.

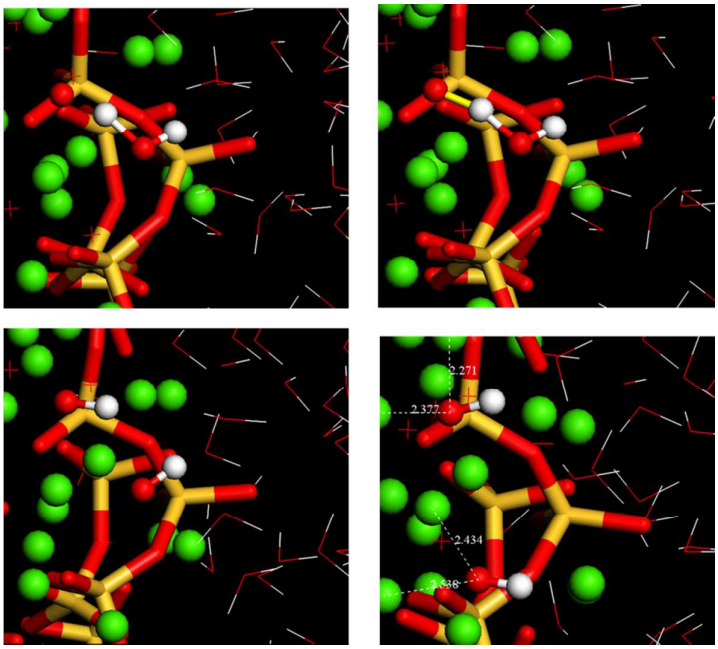

Fig.4. reaction pathway of water dissociation on the Ca-O site

3.2 Atomic profiles and dipole distribution

Atomic profiles

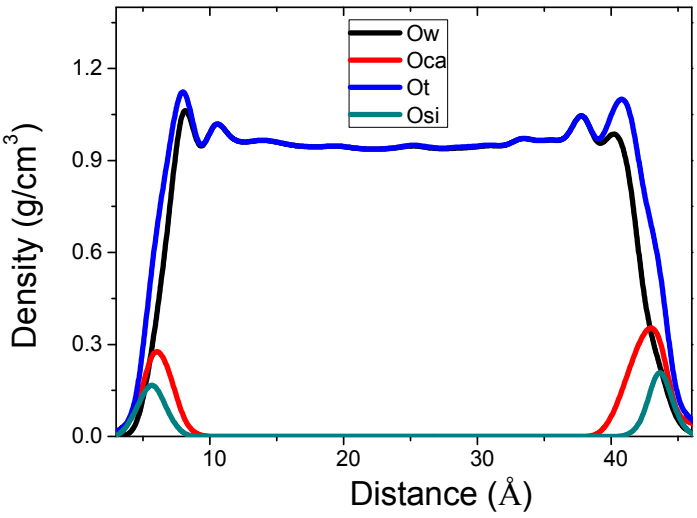

(a)

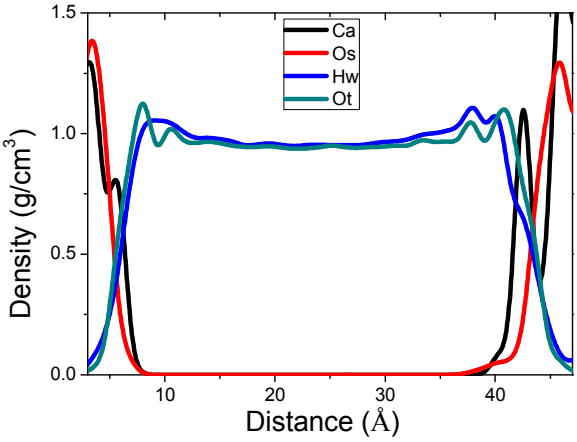

(b)

Fig.5 (a) density profile along z direction: O_w (oxygen atom in the water); O_{ca} (oxygen atom in the Ca-OH); O_{si} (oxygen atom in the Si-OH); $O_t=O_w+O_{ca}$; (b) density profile of O_t , H_w and Ca atoms.

Density profiles normal to the substrate surface were used to give first insights of the water distributions. As shown in Fig. 5a, the density profiles of oxygen atoms include the distribution of O_w, O_{si} and O_{ca}. The distribution curves for the atoms are not exactly symmetrical to the middle of the pore, implying local structural differences between the bottom and top calcium silicate interface. While the hydroxylation layer of Si-OH locates with z ranging from 3 to 8.3 Å with an average value at 5.56 Å, the Ca-OH profile has a peak at around 6.17 Å. The distributions of O_{Si} and O_{Ca} are overlapped, and the location of O_{Ca} slightly shifts away from the calcium silicate surface, indicating that the Ca-OH groups are the outmost part of the hydroxylation layer. In addition, the O_w density profile has two pronounced peaks at around 8.2 Å and 10.7 Å and oscillation becomes smaller up to 12 Å from the calcium silicate surface. As shown in Fig. 5b, even though no obvious local maximum can be observed in the hydrogen intensity profile at the downward substrate, the surface intensity is slightly increased to 1.05 g/cm^3 at 10 Å and continues decreasing to around 1 g/cm^3 around 12 Å from the surface. In compared with its crystal analogues,

oxygen and hydrogen profiles in the C-S-H gel have less shark peaks (Hou & Li, 2013). The broken silicate chains disturb arrangement of neighboring Ca atoms and further influence the order packing of surficial water molecules. As shown in Fig. 5b, the calcium atoms and the O_{NB} atoms are highly concentrated in the interface region. On the one hand, O_{NB} atoms in the dimmer structure provides large amount of H-bonds connection with neighboring water molecules. On the other hand, surface calcium atoms can strongly attract the water molecules by forming Ca-O_w bond.

Surface water organization can be well described by the atomic density contours projected in the surface plane. The trajectories of water molecules within 10 Å from calcium silicate surface are recorded in Fig. 6. As shown in Fig. 6, the triangular contours with silicon in the center are the projections of the silicate tetrahedrons and black points are the surficial calcium atoms, which are taken as the reference positions for the water trajectories.

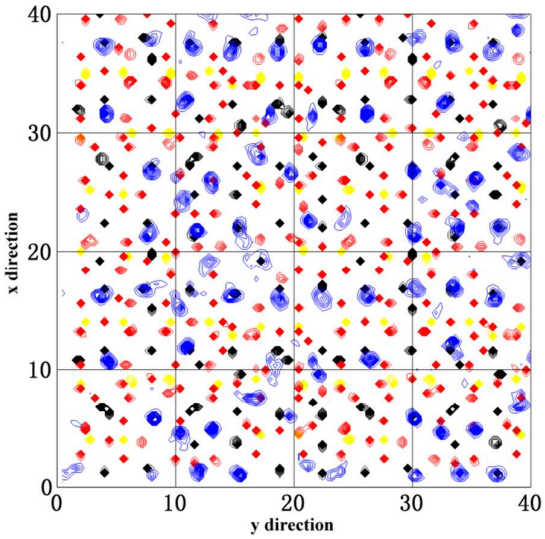

(a)

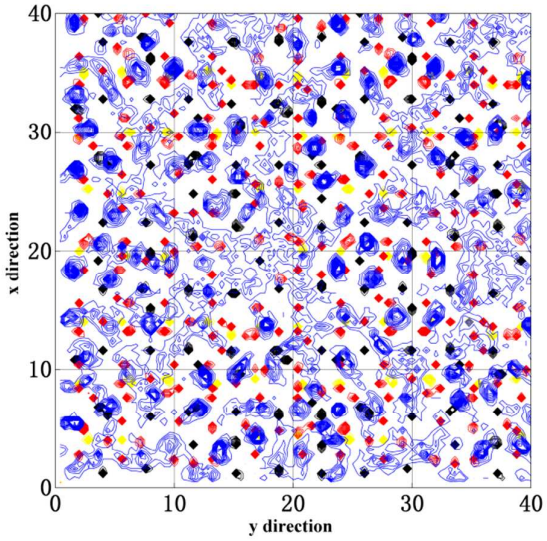

(b)

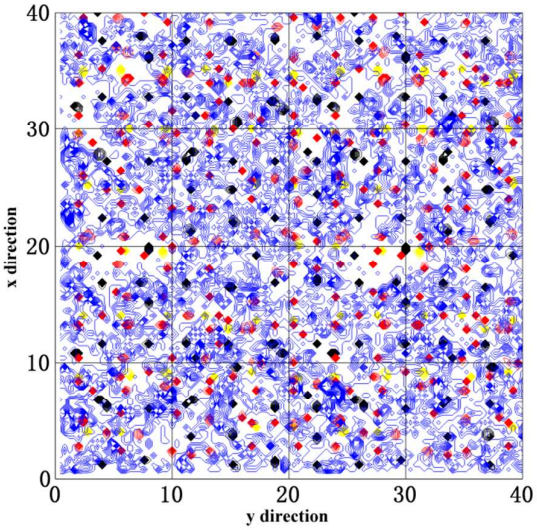

(c)

Fig.6 contour maps of O_w trajectories projected in the ***XY*** plane. Locations of each layer (a) z=5~7.5 Å (b) z=7.5 ~10 Å (c) z=10 ~12.5 Å

As shown in Fig. 6a, the water molecules and hydroxyl groups have well-ordered structures. In particular, the trajectories at x=16 Å and 38 Å shows that water molecules are distributed in a line along the silicate chain extension. It should be noted that the surficial calcium atoms, located below the water molecules, also organize along the ***y*** direction. Besides, small amount of trajectories coincide to the

location of O_{NB} atoms. It can be explained by dominant percentage of Ca-OH groups at this layer. As shown in Fig.6a, since few trajectories overlap between two neighboring water molecules, it is believed that the mobility of water molecules at this layer is relatively slow and no position exchange occurs. In the upper layer (Fig. 6b), the contours become less ordered and exchanges between the water molecules occur. The third density map (Fig. 6c) exhibits the arrangement of water molecules outside the hydroxylation layer. The less well-ordered surface water layer is also a transition zone, above which the ordered organization is difficult to be observed. The atomic trajectories from the bottom to top layers apparently show that water molecules transform from orderly organized hydroxylation layers to disordered bulk water.

Dipolar moment distribution

Dipole moment distribution of individual water molecule is utilized to characterize interaction between water molecules and the C-S-H substrate quantitatively. It should be noted that the dipole magnitude, sensitive to the local environment, turns to larger value at the hydrophilic surface, and decrease at the hydrophobic one (Youssef, et al., 2011). The dipole moment is calculated according to the method in reference (Manzano, et al., 2011). Dipole moment distribution of water molecules with different distance from the C-S-H surface is plotted in Fig.7. As shown in Fig. 7a and Fig. 7b, the mean dipole moment value of water molecules reduces from 2.4 to 2.15 D, as distance from C-S-H surface increases to 12 Å.

While the former value approximates that of water confined in the C-S-H gel, the latter one resembles the dipole moment in the bulk water (Manzano, et al., 2011). The relative large magnitude of surface water confirms the hydrophilic nature of the C-S-H surface. The large electric field at the calcium silicate surface polarizes the water molecules to an extent larger than the self-polarization in the normal liquid water. With progressively increasing distance from surface, the poling role of calcium silicate phase is weakened, gradually reducing the dipole moment.

In particular, as shown in Fig.7a and Fig. 7b, the dipolar moment of all the water layers follows the uni-modal distribution except the water molecules located at distance 6.5 to 7.5 Å from the surface, where moment is split into bimodal distribution. The special distribution mode can be explained by different polarizing effects from two different components in the calcium silicate surface. As shown in Fig. 7a, while the main peak located at 2.38 D is mainly contributed to the O_{NB} sites in the silicate chains, the slight smaller peak at around 2.91 D is due to the solvated Ca_w atoms. Since O_{NB} sites occupy the dominant percentage in the surface of C-S-H gel, the impact from the defective silicate chains is significant. However, in the layer with z from 6.5 Å to 7.5 Å, the courter-ions, Ca_w atoms, are highly concentrated and change the electronic field of surface. For example, aggregation of the Ca_w atoms neutralizes the local negativity of O_{NB} sites or even results in the local positivity. The neutralizing degree is responsible for the depolarizing role and hydrophilic nature of the C-S-H surface. The bimodal distribution is a consequence of polarization induced by both defective chains and courter-ions.

Additionally, as shown in Fig. 7c, the charge value distribution of O_w atoms located with z from 6.5 to 7.5 Å, has two peaks located at -0.78 e and -0.85 e. The charge discrepancy indicates different polarizing roles of O_{NB} sites and Ca_w atoms: the Ca_w atoms can increase the negativity of neighboring O_w atoms in greater extent than O_{NB} sites. The negativity of O_w connected with Ca_w is increased, which is consistent with previous finding by both ReaxFF simulation and ab initio calculation (Manzano, et al., 2012). In the simulation of water hydration on the calcium oxide surface, on average, O_w atoms in the $Ca{\cdot}nH_2O$ clusters (-0.82 e) have more negative charge than those in the $CaO{\cdot}nH_2O$ or $Ca(OH)_2{\cdot}nH_2O$ cluster (-0.72 to -0.75 e). It is valuable noting that reactive force field allows atomic charge to vary according to the local environment change, which is different with fixed charge simulated by the empirical water model such as TIPS (Jorgensen, 1981), SPC, TIP3P and SPC/E (Jorgensen, et al., 1983). Hence, the variable negativity of water molecules, sensitive to the local environment, help explain the polarizing effect caused by O_{NB} sites and Ca_w sites more accurately.

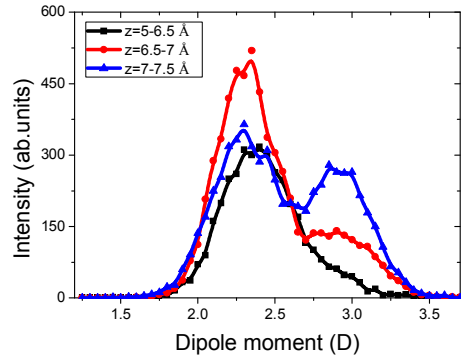

(a)

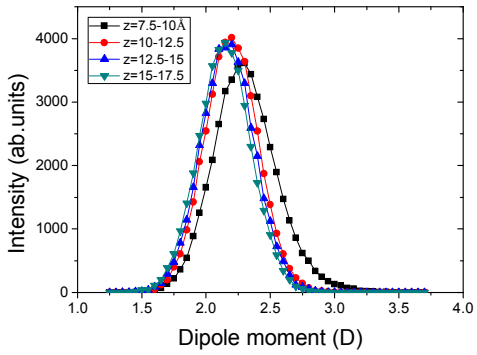

(b)

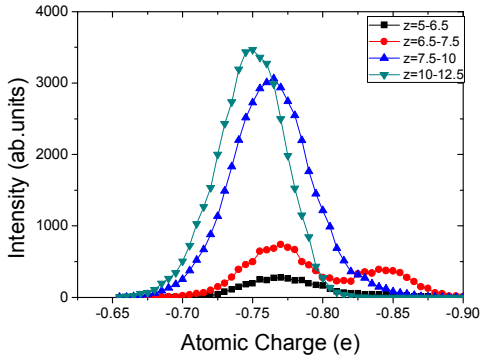

(c)

Fig.7 (a) (b) Dipolar moment distribution of water layers from 5Å to 17.5 Å; (c) O_w charge distribution of water layers from 5Å to 12.5 Å.

Orientation profiles

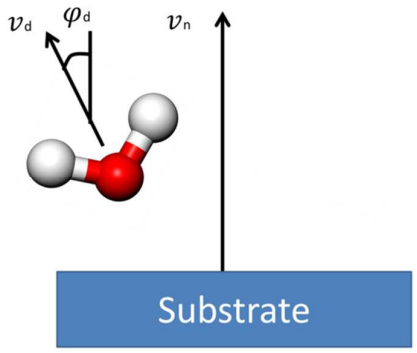

(a)

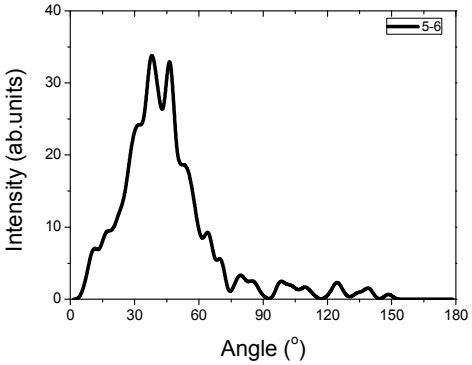

(b)

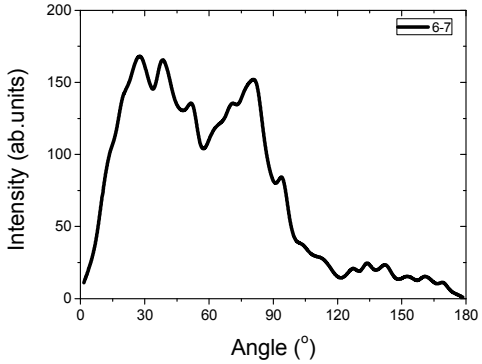

(c)

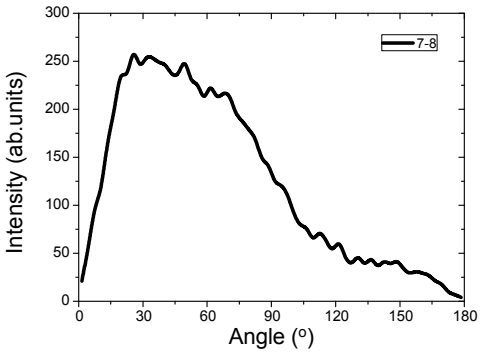

(d)

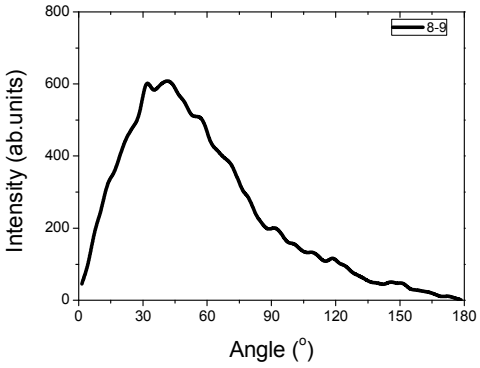

(e)

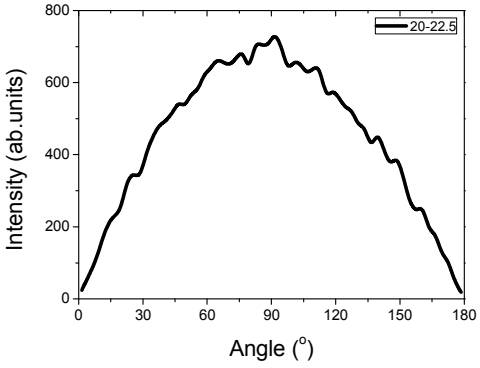

(f)

Fig.8 (a) schematic illustration of dipole moment; (b)~(f) Dipole angle distribution at different water layers. Layers locations is marked in the Fig (b) to Fig (f)

Orientation profiles, describing the dipole angle (φ_d) variation with distance from

surface, can give us better understanding of the water molecule structure in the complicated interface environment. As shown in Fig. 8(a), φ_d is the angle between the dipole vector ($\boldsymbol{\nu}_d$) of single water and the normal vector ($\boldsymbol{\nu}_n$) for the surface. Those instantaneous orientations of water molecules at different layers show different tendency that can be utilized to analyze the surface influence.

From calcium silicate surface, the orientation distribution of the water molecules is calculated every 1 Å and plotted in Fig.8 b, c, d and e. Besides, the water layer with 2.5 Å thickness located in the center of the pore is taken for comparison. In the first layer (z=5~6 Å), water molecules are, on average, deeply restricted between the silicate channel, are predominantly oriented with φ_d ranging from 37° ~ 47°, implying that dipole axis tilted away from the surface. The orientation preference can be interpreted by that oxygen atom in the water molecule is strongly adsorbed by the Ca_s atoms in the calcium silicate sheet, which can be clearly observed in Fig. 9a. The orientation of water in this layer resembles channel water molecules in the tobermorite and jennite (Hou & Li, 2013). In compared with the Ca_w atoms in the interlayer region, the Ca_s atoms in the silicate sheet are more stable. Hence, the strong Ca_s-O_w connection and the geometric restriction from the silicate channel both determine the orientation of the water molecule in this layer.

In the second layer(z=6~7Å), the orientation profile has two major peaks located at around 30° and 80° respectively, with a small shoulder ranging from 120° to 180°. The bimodal distribution, similar with the dipolar moment distribution, is also attributed to the effects from O_{NB} sites in the silicate chains, interlayer calcium atoms and hydroxyl groups. The first peak ranging from 30~37° implies the dipolar vector pointing away from surface. As shown in Fig. 9b, the O_w atoms energetically prefer the H atoms in the hydroxyl group and calcium atoms, which contribute to small dipolar angle. The small dipolar angle distribution resembles that of type II water molecules on the Mg-OH and Ca-OH interface (Wang, et al., 2004) (φ_d =30~60°).

On the other hand, Fig. 9c displays that O_{NB} atoms in the silicate chains result in the H_w-down orientation for water molecules, corresponding to the large dipolar angle distribution from 120° to 180°. As mentioned in previous simulation of interface between water molecule and hydroxylated silicate glass, water molecules have two ideal orientation styles with φ_d at 75° and 180° respectively (Lee & Rossky, 1994). Water orientation in current simulation is close to the latter style.

It should be noted that C-S-H surface after hydrolytic reaction demonstrates combining features of portlandite and silica surfaces. Water molecules located between the calcium hydroxyl and the O_{NB} atoms in the defective chains have distinguished orientation ranging from 80° to 85°. As shown in Fig. 9d, while the water molecule donates one H-bond to the O_{NB} atom, it accepts one H-bond from one Ca-OH group. It results in the dipole of water molecule pointing parallel to the C-S-H substrates.

In the further upper layer, the double peaks in the second layer emerge to wider one from 30° to 60°. In the fourth layer, the dipole angle shift toward the larger value, implying the weakening attractive role from the interlayer Ca atoms as water molecule moves away from the calcium silicate surface. As shown in Fig. 8f, since the dipole angle of water molecules depends greatly on the frequently breakage H-bonds between neighboring molecules, the water in the middle of the gel pore have no orientation preference.

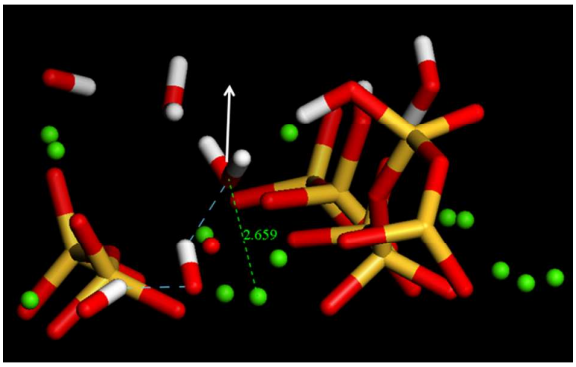

(a)

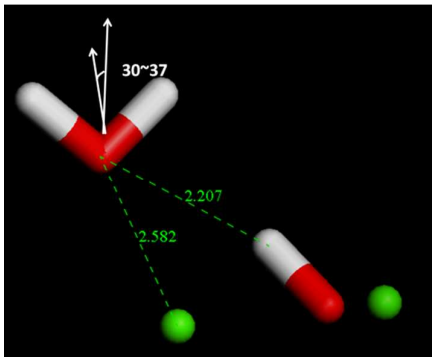

(b)

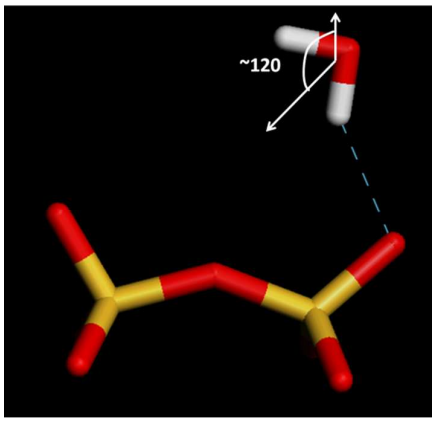

(c)

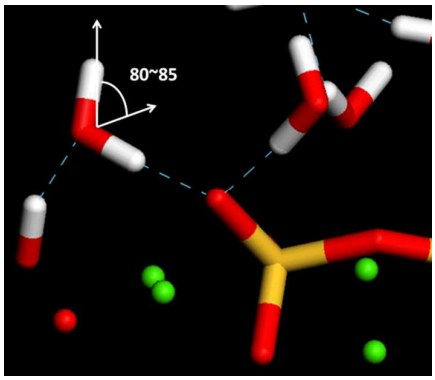

(d)

Fig.9 Snapshots of the molecular structure of water molecules with different orientation preferences. (a) water molecules located from 5 to 6.5 Å (b) (c) (d) water molecules located from 6.5 to 7.5 Å

3.3 Local structures and H-bond network

Radial distribution function

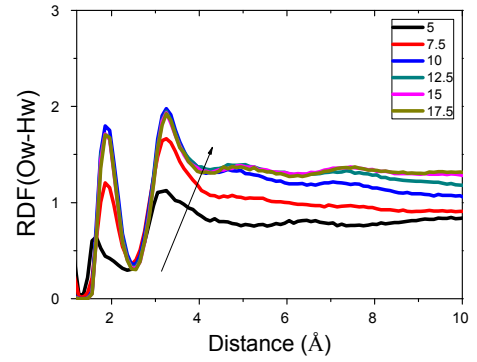

(a)

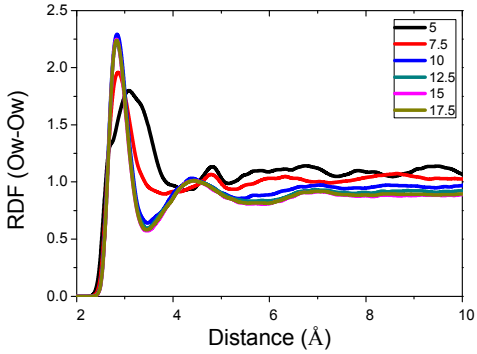

(b)

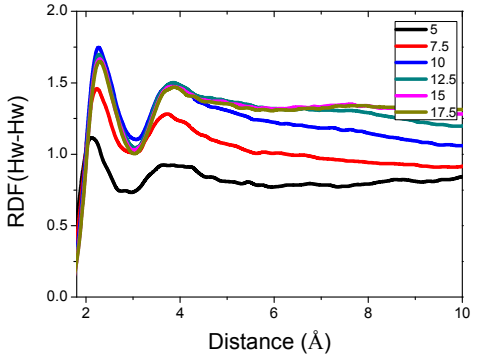

(c)

Fig.10 radial distribution function of (a) O_w-H_w (b) O_w-O_w (c) H_w-H_w for the water layers from 5 to 17.5 Å from the surface.

With distances ranging from 5 to 17.5 Å to the C-S-H substrate, radial distribution functions (RDF) of O_w-H_w, O_w-O_w and H_w-H_w are calculated and plotted in Fig.10 to describe the spatial correlation between water molecules. The height discrepancy of the peaks in RDFs of various water layers are mainly caused by the different number of molecules in each layer. On the other hand, the relative positions of local maximum and minimum, and the width of the peak are greatly influenced by the local restraints from the C-S-H substrates. As shown in Fig. 10a, as the distance increases from 5 to 17.5 Å from the C-S-H surface, the first peak of RDF (O_w-H_w), which is related to the average H-bond number, upshifts from 1.58 Å to 1.87 Å. Also, the position of the second peak slightly shifts from 3.14 to 3.24 Å. The shorter peak's location at C-S-H surface, indicating strong H-bond connectivity, is attributed to hydroxylation of water near the surface. Due to the hydrolytic reaction, part of the water molecules transforms to Ca-OH and Si-OH groups, the stronger negativity of which shorten the interatomic distance. Besides the small H-bonds distance close to the surface, the coordination number of the O_w decreases significantly, implying the reduction of the H-bonds number. It can be explained by the fact that water molecules donate part of H-bonds to the O_{NB} atoms so that the H-bond connections between neighboring water molecules are reduced. Similarly, as shown in Fig. 10c, due to the strong H-bond connectivity, the peaks of RDF (H_w-H_w) of surface water molecules also are also located at a shorter distance, in compared to those far from the C-S-H substrate.

As shown in Fig. 10b, the RDF of O_w-O_w for surface water molecules have peaks located at 3.13, 4.85, 6.8, 7.9 and 9.4 Å. The first and second peaks of RDF (O_w-O_w) shift toward lower value as the water molecules' location is far away from the C-S-H surface. It implies that the O_w-O_w correlation persists in a longer distance at the surface. Evolution of the RDF curves with distance away from the surface reflects the disturbing role that the C-S-H substrate plays in three respects: strong electronic attraction from the interlayer calcium atoms; defective silicate chains provide non-bridging sites to connect with surface water molecules by strong H-bond connectivity; the dehydration of water molecules and formation of hydroxylation

groups further change the geometry of the C-S-H substrates.

H-bonds network

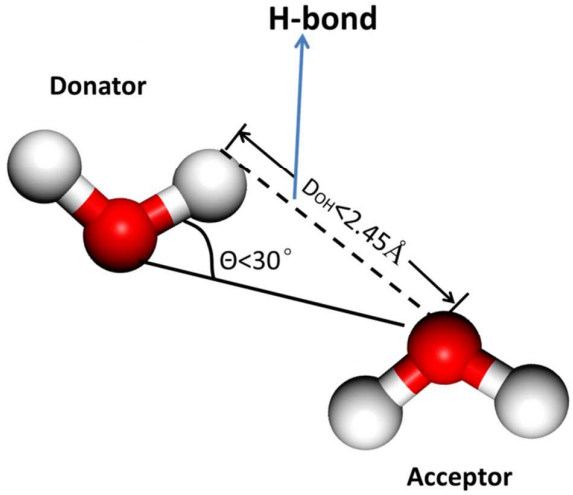

(a)

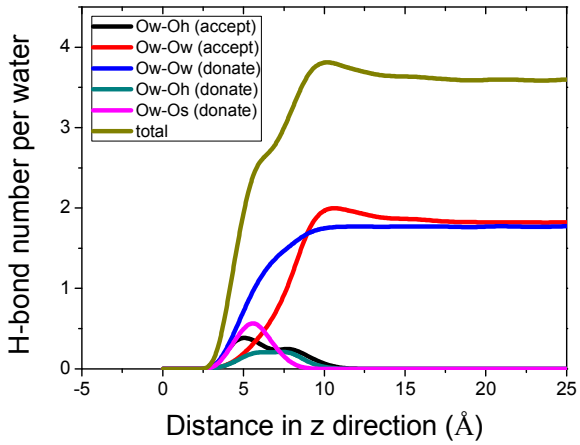

Fig.11 (a) schematic illustration of H-bonds formation; (b) H-bonds number evolution from surface

H-bond network is important to characterize the water structures and describe the interaction between substrate and neighboring water molecules. H-bond network structures are constructed by both the contribution from the water molecules and surface element. Therefore, to describe local H-bond environments, it is necessary to calculate the average H-bond numbers, the average H-bond number contributed by

the neighboring water molecule and substrate element respectively.

Fig. 11a describes the H-bond formation between two neighboring water molecules and the H-bonds formation is detected by both the angle and distance between two water molecules, as proposed by Wang et al. (Wang, et al., 2004). The H bond formation requires two conditions: two water neighbors distance D_{HO} should be less than 2.45 Å and the angle θ between the OH vector and OO vector should be less than 30°. If both conditions are satisfied, the one that provides the H atoms to form H-bond is called donator while the oxygen container is defined as the acceptor. Similarly, the substrate element can also play the role of H-bond donator or acceptor.

H-bonds connectivity between the C-S-H substrate and the near-surface water molecules is in great extent responsible for the structuring of the water molecules mentioned above. Fig. 11b shows that the average number of H-bonds per H_2O molecule first increases to 3.8 in the near-surface layer and subsequently decreases to 3.6 (approximately the value for bulk water) at 12 Å from the surface. The H-bonds number evolution resembles the variation of H-bonds in the interface between water molecules and brucite surface, but hydroxyl groups in the C-S-H surface is relative more complicated. Hence, the oscillation of the H-bond connectivity is categorized into five components to distinguish the donating or accepting role as well as the different interactions from neighboring water molecules or from OH groups.

For the water molecules located from 5 to 6.5 Å, on average, the water molecule donate 1.02 H-bonds to surrounding water molecules and 0.9 H-bonds to the OH groups and O_{NB} in the silicate chains, but only accept less than 0.68 H-bonds from neighboring water molecules and C-S-H substrate. The large percentage of the water donator is due to lots of O_{NB} sites in the defective silicate chains. Besides, the calcium atoms also influence the H-bonds structuring. As shown in Fig. 9a, water molecules is the coordinated atom for the bottom calcium atoms, which result in the dipole of water molecules pointing upward. In this respect, they are more probable to donate

H-bonds to the up layer water molecules.

In the layer located from 6.5 Å to 7.5 Å, while the average H-bond number donated by water molecule and OH groups is 1.85, the H-bond number accepted is around 0.9. While the ratio of water donator decreases, the acceptor's ratio increases in some extent. The changes of acceptor and donators are caused by the variation of the molecular structure in C-S-H substrate. On one hand, due to the reduction of O_{NB} atoms, less number of H-bonds can be accepted by the O_{NB} sites. The Ca_w atoms, connecting with the O_{NB} atoms, neutralize the negativity of the defective silicate chains and further prevent the water molecules from donating H-bonds. On the other hand, due to the hydrolytic reaction, a lots of O_{NB} site transform to the hydroxyl groups. The hydroxyl groups can both serve as H-bonds acceptor and donator, which further reduce the probability of water donators.

In the upper layer from 7.5 to 10 Å, the outmost of the hydroxylation layer, 1.8 H-bonds accepted from neighboring water molecules and 1.7 H-bonds donated from the water molecules, as well as 0.2 H-bonds connected with OH groups, contribute to 3.7 H-bonds connection. In this layer, the number of water donator further decreases and the accepted H-bonds number turns to be larger than the donated one, which is caused by decreasing number of O_{NB} in this region as displayed in Fig.11b. Even though the total number of H-bonds increases, the percentage of the connectivity with O_h and O_{NB} reduce significantly. Since the bond strength of O_{NB}-O_w is far better than that of O_w-O_w (Youssef, et al., 2011), the stability of this layer transforms to more unstable. It explains the loose and disordered atomic trajectories of water molecules in this layer as shown in Fig.6.

3.4 Dynamic properties

In addition to the structures features, the mobile properties of water confined in the nano pore are also significantly influenced by the solid-water interface. The mean

square displacement MSD (t) and diffusion coefficient (D) (Kerisit & Liu, 2009), a parameter to estimate the dynamic properties of water molecules, can be defined by Eq.,

$$\mathrm{MSD(t)} = < |\boldsymbol{r_i}(\mathrm{t}) - \boldsymbol{r_i}(0)|^2 > \quad (1)$$

$$2\mathrm{D} \cdot \mathrm{t} = \frac{1}{n} < |\boldsymbol{r_i}(\mathrm{t}) - \boldsymbol{r_i}(0)|^2 > \quad (2)$$

where $\boldsymbol{r_i(t)}$ represents the position of atom *i* at time t , $\boldsymbol{r_i(0)}$ is the original position of atom *i* . MSD takes into account 3-dimensional coordinates for the bulk water molecules in ***x***, ***y*** and ***z*** directions, 2-dimensional coordinates parallel to the C-S-H substrate and 1-dimensional coordinate perpendicular to the C-S-H substrate.

As shown in Fig.12a, for the water molecules confined in the gel pore, the mean square displacement shows three stages. In the first 1 Ps, MSD varies in a parabolic mode from 0 to 2 $Å^2$. In the initial stage, small motions of water molecules indicate slight influence by neighboring atoms. The surface water dissociation happens frequently, which results in the fluctuation of the MSD curve. Subsequently, the MSD increases slowly and step into a cage stage. Not like the structural water molecules in the C-S-H gel, the cage regime remains in a shorter time less than 10 Ps (Youssef, et al., 2011) (Qomi, et al., 2014). The restriction from the defective silicate chains and interlayer calcium atoms is relative weaker in compared to that of the ultra-confined pore with width less than 1 nm. Hence, it takes less time for the surficial water molecules to escape from constraints from neighboring atoms. Finally, after 10 Ps, the MSD curve moves to the diffusion stage, where the MSD is proportional to t. Furthermore, the MSD values parallel to the C-S-H gel substrate are slightly larger than those perpendicular to the substrate. In the diffusion stage, the MSD_{xy} curve almost coincides with MSD in three dimensions, but the MSD_z curve turns to lower value, which reflects the geometrical and electronic confinement of the nano-pore.

To further evaluate the diffusivity of the water molecules, MSD values of O_H in the

hydroxylation layers and O_w in the water molecules are calculated. As shown in Fig. 12b, the mobile ability of hydroxyl groups embedded in the C-S-H surface is reduced significantly in compared with gel pore water molecules. It takes more than 200 ps for the O_H atoms to displace about 1 $Å^2$ in the caging stage, implying similar dynamical behavior with water molecule in the ice-state. The ice-like hydroxyl groups can explain the condensed trajectories in the atomic profiles in ***XY*** plane: only vibrations and restricted rotations, rather than diffusion, are the available movement of hydroxyl groups. Hence, water dissociation near the surface help construct a stable and rigid hydroxylation layer with glassy nature of structural water molecules ultra-confined in the C-S-H gel.

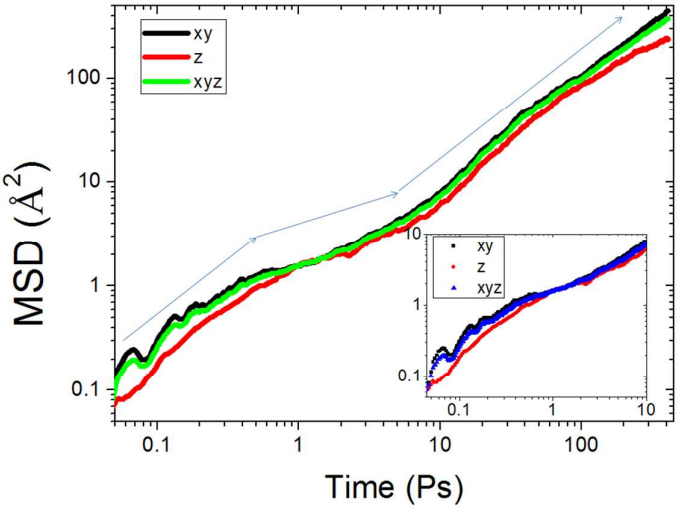

(a)

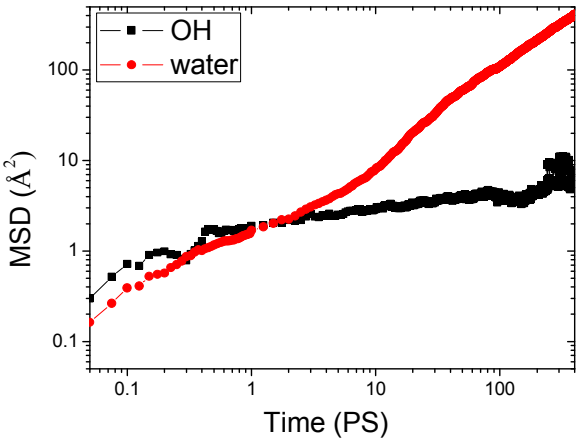

(b)

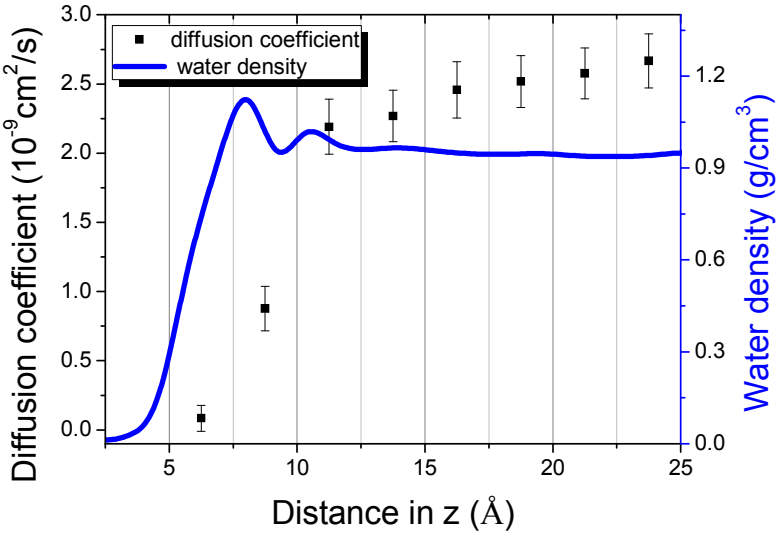

(c)

Fig. 12 (a) diffusion coefficient of water confined in the C-S-H gel (Dxyz) and its component parallel to the C-S-H surface (Dxy) and normal to the C-S-H surface (Dz); (b) diffusion coefficient of hydroxyl groups and surface water molecules. (c) diffusion coefficient evolution with distance from the surface.

In addition, water region is divided into several layers parallel to surface with width 2.5Å. Diffusion coefficient is calculated for each individual layer. It can be observed from Fig.11c that with progressively increasing from surface, the diffusion coefficient gradually increases and only when the water moves more than 15 Å from surface, the water diffusion coefficient approximates value in bulk water (experimental value of D_{H2O} about 2.66 $\times$ 10^{-9} m^2/s (Jones, et al., 1965)).

D_{xyz} for water molecules in the first and second layer are 0.08 and 0.8 $\times$ 10^{-9} m^2/s respectively. The former one is in the magnitude of the diffusion coefficient of water between the C-S-H particles tested by a proton field cycling relaxometry approach (PFCR) (D=1/80 D_{H2O}) (Korb, et al., 2007) and Time-Resolved Incoherent Elastic Neutron Scattering (D=1/6 D_{H2O}) (Fratini, et al., 2013). Because the PFCR technique is developed to detect dynamical properties of water molecules adsorbed on the pore

surface, MD simulation by reactive force field confirms the effectiveness of the experimental techniques. Furthermore, combined with previous structural and bond analysis, the reasons for low diffusion coefficient of the surface water molecules can be attributed to three aspects. First, due to the high reactivity of the C-S-H surface, part of water molecules transform to the "immobile" structural phase. Secondly, due to the large amount of O_{NB} sites in the silicate chains, O_w-O_{NB} H-bonds in the interface region become the dominant connectivity that constrains the mobile ability of surface water molecules. Another important factor is the solvated cation ions, Ca_w atoms, whose coordinated water molecules diffuse slowly due to the strong electronic attraction.

4. Conclusion

In light of the molecular dynamics by the reactive force field, the reactivity, structures and dynamics properties of water confined in the C-S-H gel pore have been investigated. Several conclusions can be drawn from this study as follows:

(1) Due to the high reactive C-S-H surface, hydrolytic reactions happens in the solid-liquid interfacial zone and partial surface adsorbed water molecules transforming to the Si-OH and Ca-OH groups strongly embedded in the C-S-H structure.

(2) Because of the electronic discrepancy, silicate and calcium hydroxyl groups result in the binomial distribution of dipolar moment and water orientation. While the Ca-OH contributes to O_w-downward orientation, the O_{NB} atoms in the silicate chains prefer accepting H-bonds from surface water molecules.

(3) Furthermore, the defectives silicate chains and solvated Ca_w atoms near the surface contribute to the glassy nature of surface water: large packing density, pronounced orientation preference, and distorted organization.

(4) The stable H-bonds connected with Ca-OH and Si-OH groups also restrict the mobility of the surface water molecules. The diffusion coefficient of surface water molecules (0.08 and 0.8 $\times$ 10^{-9} m^2/s) matches well with the experimental results obtained by NMR, QENS and PCFR techniques.

Acknowledgement

Financially support from the China Ministry of Science and Technology under Grant 2015CB655100, Major International Joint Research Project under Grant 51420105015 and National Natural Science Foundation of China under Grant 51278260 are gratefully acknowledged.

References

Bonnaud, P. A. et al., 2012. Thermodynamics of Water Confined in Porous Calcium-Silicate-Hydrates. *Langmuir ,* 28(31), p. 11422−11432.

Bordallo, H. N., Aldridge, L. P. & Desmedt, A., 2006. Water dynamics in hardened ordinary portland cement paste or concrete: from quasielastic neutron scattering. *Journal of Physics and Chemistry B ,* 110(36), pp. 17966-17976.

Brenner, D. W. et al., 2002. A second-generation reactive empirical bond order (REBO) potential energy expression for hydrocarbons. *Journal of Physics: Condensed Matter,* 14(4), pp. 783-802.

Brough, A., Dobson, C., Richardson, I. & Groves, G., 1994. In situ solid-state NMR studies of Ca_3SiO_5: hydration at room temperature and at elevated temperatures using ^{29}Si enrichment. *Journal of Materials Science ,* 29(15), pp. 3926-3940.

Cong, X. & Kirkpatrick, R., 1996. ^{29}Si MAS NMR study of the structure of calcium silicate hydrate. *Advanced Cement Based Material,* 3(3-4), pp. 144-156.

Cygan, R. T., Liang, J. J. & Kalinichev, A. G., 2004. Molecular models of hydroxide, oxyhydroxide, and clay phases and the development of a general force field. *The*

Journal of Physical Chemistry B, 108(4), pp. 1255-1266.

Dolado, J. S., Griebel, M. & Hamaekers, J., 2007. A Molecular Dynamic Study of Cementitious Calcium Silicate Hydrate (C-S-H) gels. *Journal of the American Ceramic Society,* 90(12), pp. 3938-3942.

Fratini, E. et al., 2013. Hydration Water Dynamics in Tricalcium Silicate Pastes by Time-Resolved Incoherent Elastic Neutron Scattering. *The Journal of Physical Chemistry C,* 117(14), pp. 7358-7364.

Greener, J. et al., 2000. Monitoring of hydration of white cement paste with proton NMR spin–spin relaxation. *Journal of the American Ceramic Society,* 83(3), pp. 623-627.

Hou, D. & Li, Z., 2013. Molecular Dynamics Study of Water and Ions Transport in Nano-Pore of Calcium Silicate Phase: A Case Study of Jennite. *Journal of Materials in Civil Engineering,* 26(5), pp. 930-940.

Jones, J. R., Rowlands, D. L. G. & Monk, C. B., 1965. Diffusion coefficient of water in water and in some alkaline earth chloride solutions at 25° C. *Transactions of the Faraday Society,* Volume 61, pp. 1384-1388.

Jorgensen, W. L., 1981. Quantum and statistical mechanical studies of liquids. 10. Transferable intermolecular potential functions for water, alcohols, and ethers. Application to liquid water. *Journal of the American Chemical Society,* 103(2), pp. 335-340.

Jorgensen, W. L. et al., 1983. Comparison of simple potential functions for simulating liquid water. *The Journal of chemical physics,* 79(2), pp. 926-935.

Kalinichev, A. G. & Kirkpatrick, R. J., 2002. Molecular Dynamics Modeling of Chloride Binding to the Surfaces of Calcium Hydroxide, Hydrated Calcium Aluminate, and Calcium Silicate Phases. *Chemistry of Materials,* 14(8), pp. 3539-3549.

Kalinichev, A. G., Wang, J. & Kirkpatrick, R. J., 2007. Molecular dynamics modeling of the structure, dynamics and energetics of mineral water interfaces: application to cement materials. *Cement and Concrete Research,* 37(3), pp. 337-347.

Kerisit, S. & Liu, C. X., 2009. Molecular simulation of water and ion diffusion in

nanosized mineral fractures. *Environmental Science and Technology,* 43(3), pp. 777-782.

Korb, J. P., Monteilhet, L., McDonald, P. J. & Mitchell, J., 2007. Microstructure and texture of hydrated cement-based materials: A proton field cycling relaxometry approach. *Cement and Concrete Research,* 37(3), pp. 295-302.

Lau, T., Kushima, A. & Yip, S., 2010. Atomistic Simulation of Creep in a Nanocrystal. *Physical Review Letters,* 104(17), p. 175501.

Lee, S. H. & Rossky, P. J., 1994. A comparison of the structure and dynamics of liquid water at hydrophobic and hydrophilic surfaces—a molecular dynamics simulation study. *The Journal of Chemical Physics,* 100(4), pp. 3334-3345.

Leroch, S. & Wendland, M., 2012. Simulation of Forces between Humid Amorphous Silica Surfaces: A comparison of empirical atomic force fields. *The Journal of Physical Chemistry C,* 116(50), pp. 26247-26261.

Manzano, H., Masoero, E., Arbeloa, I. & Jennings, H., 2013. Molecular modelling of shear deformations in ordered and disordered Calcium Silicate Hydrates. *Soft Matter,* 9(30), pp. 7333-7341.

Manzano, H. et al., 2011. Confined Water Dissociation in Microporous Defective Silicates:Mechanism, Dipole Distribution, and Impact on Substrate Properties. *Journal of the American Chemical Society,* 134(4), p. 2208−2215.

Manzano, H., Pellenq, R., Ulm, F. & Buehler, M., 2012. Hydration of Calcium Oxide Surface Predicted by Reactive Force Field Molecular Dynamics. *Langmuir,* 28(9), pp. 4187-4197.

Murray, S. J., Subramani, V. J., Selvam, R. P. & Hall, K. D., 2010. Molecular Dynamics to Understand the Mechanical Behavior of cement Paste. *Journal of the transportation Research Board,* 2142(11), pp. 75-82.

Pellenq, R. J. et al., 2009. A realistic molecular model of cement hydrates. *PNAS,* 106(38), p. 16102–16107.

Puibasset, J. & Pellenq, R., 2008. Grand Canonical Monte Carlo Simulation Study of Water Adsorption in Silicalite at 300 K. *The Physical and Chemistry B,* 112(20), pp. 6390-6397.

Qomi, M. J. A., Bauchy, M., Ulm, F. J. & Pellenq, R. J. M., 2014. Anomalous composition-dependent dynamics of nanoconfined water in the interlayer of disordered calcium-silicates. *The Journal of Chemical Physics,* 140(5), p. 054515.

Rakiewicz, E. F., Benesi, A. J., Grutzeck, M. W. & Kwan, S., 1998. Determination of the state of water in hydrated cement phases using deuterium NMR spectroscopy. *Journal of the American Chemical Society,* 120(25), pp. 6415-6416.

van Duin, A. et al., 2003. ReaxFFsio Reactive Force Field for Silicon and Silicon Oxide Systems. *The Journal of Physical Chemistry A,* 107(19), pp. 3803-3811.

Wang, J. W., Kalinichev, A. G. & Kirkpatrick, R. J., 2004. Molecular modeling of water structure in nano-pores between brucite (001) surfaces. *Geochimica et Cosmochimica Acta,* 68(16), pp. 3351-3365.

Wang, P. S. et al., 1998. 1H nuclear magnetic resonance characterization of Portland cement: molecular diffusion of water studied by spin relaxation and relaxation time-weighted imaging. *Journal of Material Science,* 33(12), pp. 3065-3071.

Youssef, M., Pellenq, R. J. M. & Yildiz, B., 2011. Glassy Nature of Water in an Ultraconfining Disordered Material:The Case of Calcium silicate hydrate. *Journal of the American Chemical Society,* 133(8), p. 2499–2510.

Yu, P. & Kirkpatrick, R. J., 2001. 35Cl NMR relaxation study of cement hydrate suspensions. *Cement and Concrete Research,* 31(10), p. 1479—1485.